Title

Development of a Mouse Model of Metabolic Syndrome, Pulmonary Hypertension, and Heart Failure with Preserved Ejection Fraction

Journal

American Journal of Respiratory Cell and Molecular Biology, 56(4)

ISSN

1044-1549

Authors

Meng, Qingqing
Lai, Yen-Chun
Kelly, Neil J
et al.

Publication Date

2017-04-01

DOI

10.1165/rcmb.2016-0177oc

Peer reviewed

ORIGINAL RESEARCH

Development of a Mouse Model of Metabolic Syndrome, Pulmonary Hypertension, and Heart Failure with Preserved Ejection Fraction

Qingqing Meng[1,2], Yen-Chun Lai[1,3], Neil J. Kelly[3], Marta Bueno[1,3], Jeffrey J. Baust[1], Timothy N. Bachman[1], Dmitry Goncharov[1], Rebecca R. Vanderpool[1], Josiah E. Radder[3], Jian Hu[1], Elena Goncharova[1,3], Alison M. Morris[3], Ana L. Mora[1,3], Steven D. Shapiro[3], and Mark T. Gladwin[1,3]

[1]Pittsburgh Heart, Lung, Blood, and Vascular Medicine Institute, University of Pittsburgh, Pittsburgh, Pennsylvania; [2]School of Medicine, Tsinghua University, Beijing, China; [3]Division of Pulmonary, Allergy and Critical Care Medicine, University of Pittsburgh, Pittsburgh, Pennsylvania

Abstract

Pulmonary hypertension (PH) associated with heart failure with preserved ejection fraction (PH-HFpEF; World Health Organization Group II) secondary to left ventricular (LV) diastolic dysfunction is the most frequent cause of PH. It is an increasingly recognized clinical complication of the metabolic syndrome. To date, no effective treatment has been identified, and no genetically modifiable mouse model is available for advancing our understanding for PH-HFpEF. To develop a mouse model of PH-HFpEF, we exposed 36 mouse strains to 20 weeks of high-fat diet (HFD), followed by systematic evaluation of right ventricular (RV) and LV pressure–volume analysis. The HFD induces obesity, glucose intolerance, insulin resistance, hyperlipidemia, as well as PH, in susceptible strains. We observed that certain mouse strains, such as AKR/J, NON/shiLtJ, and WSB/EiJ, developed hemodynamic signs of PH-HFpEF. Of the strains that develop PH-HFpEF, we selected AKR/J for further model validation, as it is known to be prone to HFD-induced metabolic syndrome and had low variability in hemodynamics. HFD-treated AKR/J mice demonstrate reproducibly higher RV systolic pressure compared with mice fed with regular diet, along with increased LV end-diastolic pressure, both RV and LV hypertrophy, glucose intolerance, and elevated HbA1c levels. Time course assessments showed that HFD significantly increased body weight, RV systolic pressure, LV end-diastolic pressure, biventricular hypertrophy, and HbA1c throughout the treatment period. Moreover, we also identified and validated 129S1/SvlmJ as a resistant mouse strain to HFD-induced PH-HFpEF. These studies validate an HFD/AKR/J mouse model of PH-HFpEF, which may offer a new avenue for testing potential mechanisms and treatments for this disease.

Keywords: pulmonary hypertension; group 2 pulmonary hypertension; AKR/J; metabolic syndrome; pulmonary hypertension–heart failure with preserved ejection fraction

Pulmonary hypertension (PH) secondary to left heart disease (PH-LHD; World Health Organization group II) is the most frequent cause of PH worldwide, and occurs in patients with left ventricular (LV) systolic dysfunction, LV diastolic dysfunction, and valvular heart disease (1–3). With chronic elevated filling pressures in the LV caused by LHD, the backward pressure to pulmonary arteries can lead to vascular remodeling and increased pulmonary arterial pressures (PAP), pulmonary vascular resistance (PVR), transpulmonary pressure gradients, and secondary right ventricular (RV) hypertrophy (4). Epidemiological studies have documented that PH attributable to LV diastolic dysfunction, also referred to as PH associated with heart failure with preserved ejection fraction (PH-HFpEF), is more prevalent than other forms of PH-LHD.

(Received in original form June 7, 2016; accepted in final form December 30, 2016)

This work was supported by National Institutes of Health grants 2P01HL103455 (M.T.G., A.L.M., and S.D.S.), and a China Scholarship Council Fellowship (Q.M.).

Author Contributions: Experimental conception and design—Q.M., Y.-C.L., N.J.K., M.B., J.E.R., A.M.M., A.L.M., S.D.S., and M.T.G.; data collection: Q.M., Y.-C.L., N.J.K., M.B., J.J.B., D.G., J.E.R., and J.H.; data analysis and interpretation—Q.M., Y.-C.L., N.J.K., M.B., T.N.B., R.R.V., E.G., A.L.M., and M.T.G.; manuscript drafting—Q.M., Y.-C.L., and M.T.G.; all the authors have given approval of the final manuscript.

Correspondence and requests for reprints should be addressed to Mark T. Gladwin, M.D., 1218 Scaife Hall, 3550 Terrace Street, Pittsburgh, PA 15261. E-mail: gladwinmt@upmc.edu

This article has an online supplement, which is accessible from this issue's table of contents at www.atsjournals.org

Am J Respir Cell Mol Biol Vol 56, Iss 4, pp 497–505, Apr 2017

Originally Published in Press as DOI: 10.1165/rcmb.2016-0177OC on January 24, 2017
Internet address: www.atsjournals.org

Clinical Relevance

In this work, we screened the response to high-fat diet (HFD)–induced pulmonary hypertension (PH) across 36 mouse strains and identified AKR/J as a highly susceptible mouse strain. This HFD/AKR/J mouse model recapitulates key clinical features known to be present in patients with PH and heart failure with preserved ejection fraction (PH-HFpEF), including elevated right ventricular systolic pressure and left ventricular end-diastolic pressure, preserved left ventricular ejection fraction, and biventricular hypertrophy. Moreover, this mouse model was further validated on the basis of reliability and reproducibility in multiple experimental sets, including time course analysis. We believe that these findings are of significant importance, as there is no approved specific therapy and no consensus therapeutic strategy for PH-HFpEF at present. The newly developed HFD/AKR/J mouse model of PH-HFpEF may be useful for advancing our understanding and testing potential treatments for PH-HFpEF.

A recent observational study demonstrated that, among 455 patients with HFpEF characterized by LV end-diastolic pressure (LVEDP) greater than 15 mm Hg and LV ejection fraction (LVEF) of 50% or greater, 239 patients (53%) had PH, defined by a mean PAP greater than 25 mm Hg (5). Elevated pulmonary pressures are observed in 44 and 69% of patients with HFpEF according to the New York Heart Failure Registry and the Pulmonary Hypertension Connection Registry, respectively (6, 7). Currently, the hemodynamic definition of pulmonary vascular remodeling in PH-HFpEF is under debate, with the severity quantified by increased transpulmonary gradient, PVR, and/or the diastolic pressure gradient. Using the most stringent definition of an increase in the diastolic pressure gradient of 7 mm Hg or greater, the prevalence is approximately 5% of patients with LHD (8, 9). Because approximately one-half of six million heart failure patients in the United States have HFpEF (10, 11), and the presence of PH is associated with worse outcomes and mortality in patients with HFpEF (12–14), PH-HFpEF is now the subject of active investigations. Despite this, no specific therapy has been identified, and no preclinical mouse models have been developed.

Features of metabolic syndrome, including obesity, diabetes, hyperlipidemia, and hypertension, are recognized as risk factors for developing PH-HFpEF (6, 15, 16). In fact, two or more of these features are commonly seen in patients with PH-HFpEF (17). Recently, our group has developed a rat model of PH-HFpEF, which combines endothelial injury using vascular endothelial growth factor receptor blocker, SU5416, in rats with multiple features of metabolic syndrome due to double leptin receptor defect (obese ZSF1) (18). Although this SU5416/obese ZSF1 rat model closely recapitulates the cardiac phenotype of human PH-HFpEF, the rat model is expensive, with limited molecular tools and techniques compared with mice. In this work, we sought to develop a mouse model of metabolic syndrome–associated PH-HFpEF in hopes of enabling the use of genetically modifiable models for testing disease mechanism and potential treatments for PH-HFpEF. Some of the results of these studies have been previously reported in abstract form (19–21).

Materials and Methods

Animals Studies

All experimental procedures were approved by the University of Pittsburgh Institutional Animal Care and Use Committee (Pittsburgh, PA). Male mice (Jackson Laboratory, Bar Harbor, ME) were fed a high-fat diet (HFD; 60% lipids/kcal; Research Diets, New Brunswick, NJ) or regular diet (RD; 15% lipids/kcal) for 16–20 weeks, beginning at 6–12 weeks of age. Mice ($n = 3$/cage) were given free access to food and water. Body weights and health condition were monitored throughout the treatment period.

Glucose Tolerance and HbA1C Test

For glucose tolerance testing, mice were fasted for 6 hours before being subjected to intraperitoneal injection with filter-sterilized 1.8 mg/g dextrose in 0.9% NaCl. Blood samples were taken at different time points, as indicated, and blood glucose levels were measured with a portable glucose meter (ACCU-CHECK Aviva; Roche, Indianapolis, IN). HbA1c levels were determined using an HbA1c blood monitor (A1c Now+; Bayer, Whippany, NJ).

Hemodynamic and Ventricular Measurements

Mice were weighed and anesthetized with isoflurane (5% for induction, 2% during surgery, and 1% while performing pressure–volume loop measurements). RV systolic pressure (RVSP), LVEDP, and LVEF were measured by using a four-electrode pressure–volume catheter (Scisense, London, ON, Canada) attached to the data acquisition system (EMKA Instruments, Falls Church, VA). RV and LV weights normalized to tibial length were used as indexes of ventricular mass. Fulton index (weight of RV/weight of LV + septum) was used as an index of RV hypertrophy.

Pulmonary Vascular Morphometry

Lungs were perfused and fixed with 2% paraformaldehyde, followed by a 30% sucrose-PBS incubation overnight. Frozen sections (7 μm) were stained with FITC-conjugated α-smooth muscle actin (Sigma-Aldrich, St. Louis, MO) and 4′,6-diamidino-2-phenylindole. Images of terminal arterioles were captured using a fluorescence microscope digital camera system (Provis; Olympus, Tokyo, Japan). ImageJ 1.45s software (NIH, Bethesda, MD) was used to measure external diameter and medial wall thickness in 5–10 terminal arteries (ranging in size from 50 to 100 μm in external diameter) per lung section from eight mice per group. Medial index (%) = (mean medial wall thickness/mean external diameter) × 100.

Statistical Analysis

Statistical analysis was performed using GraphPad Prism 6.0 software (La Jolla, CA). Statistical significance of our data was determined by Mann–Whitney U test. Values of P less than 0.05 were considered statistically significant.

Overlapping Publication

The fold change in RV maximum pressure with high-fat feeding by background strain is also reported in an article by Kelly and colleagues (22) to identify genes associated with the development of PH (Figure 1 and set 1

in Figure E1 in the online supplement only; all other data were collected independently for further HFD/AKR/J model development and validation).

Results

Response to HFD-Induced PH across 36 Strains of Mice

Epidemiological studies indicate that patients with PH-HFpEF have a higher prevalence of hypertension, diabetes mellitus, obesity, and coronary artery disease than patients with pulmonary arterial hypertension (PAH) (6). To explore potential mouse models that can recapitulate the pathogenesis and outcome of human PH-HFpEF, we exposed mice at 6–12 weeks of age across 36 inbred and wild-derived mouse strains to RD (15% lipids/kcal) or HFD (60% lipids/kcal), which induces obesity, glucose intolerance, insulin resistance, hyperlipidemia, as well as PH (23, 24). Using right heart catheterization, we found that 12 out of 36 mouse strains tested had more than a 20% increase of RVSP after 20 weeks of HFD treatment as compared with mice fed a RD (Figure 1). Among these strains, AKR/J, NON/shiLtJ, and WSB/EiJ were highly susceptible to HFD-induced PH, suggesting that these strains may be considered as the starting points to develop metabolic syndrome–associated PH-HFpEF. Moderate changes in RVSP were seen in the most widely used inbred strain, C57BL/6J, and several related mouse strains, including C57BL/10J, C57L/J, and C57BR/cdJ. In addition, we also observed that 10 out of 36 mouse strains, such as 129S1/SvlmJ, PL/J, DBA/1J, and NOD/ShiLtJ, were relatively resistant to HFD-induced PH. *See* Kelly and colleagues (22) for detailed body weight, LVEDP, arterial blood pressure, LV mass, and RV mass across all 36 mouse strains.

Validation of HFD-Induced PH-HFpEF in AKR/J Mouse

From the strains that are highly susceptible to HFD-induced PH, we selected AKR/J for further model development as it is known to be prone to HFD-induced metabolic syndrome (25), is less aggressive, and exhibited highly reproducible hemodynamics (Figure E1). Concomitant with elevated RVSP (28.5 ± 0.7 and 37.1 ± 1.2 mm Hg, RD and HFD, respectively; mean PAP, 19.8 ± 0.3 versus 25.9 ± 0.9 mm Hg; Figure E2A), HFD-treated AKR/J mice had higher LVEDPs and preserved LVEF compared with mice treated with RD (Figures 2A-2D). In addition, both RV and LV hypertrophy were observed in HFD-treated AKR/J mice (Figures 2E and 2F).

Pulmonary vascular proliferative remodeling and elevated PVR were also observed in HFD-treated AKR/J mice (Figures 2G and 2H). Consistent with the previous studies, which described the impact of HFD on metabolic syndrome, HFD-treated AKR/J mice had significantly higher body weights and glycated hemoglobin (HbA1c) levels than RD-treated mice (Figures 2I and 2J). Moreover, as shown in Figure 2K, HFD-treated AKR/J mice had impaired glucose tolerance as determined by the glucose tolerance test. Furthermore, RVSP, LVEDP, and biventricular hypertrophy correlated with body weight and HbA1c levels in AKR/J mice (Figures 3A-3H). Collectively, these observed hemodynamic and metabolic features in HFD-treated AKR/J mice are consistent with the clinical characteristics of human PH-HFpEF.

HFD Promotes Progression of PH-HFpEF in AKR/J Mouse

To further evaluate the impact of HFD on disease progression, we monitored metabolic and hemodynamic changes in AKR/J mice throughout the treatment period. AKR/J mice consuming HFD increased their body weights compared with RD-treated mice in a time-dependent manner (Figure 4A). Consumption of HFD markedly increased HbA1c levels in AKR/J mice, particularly after 12 weeks of treatment (Figure 4B). In line with

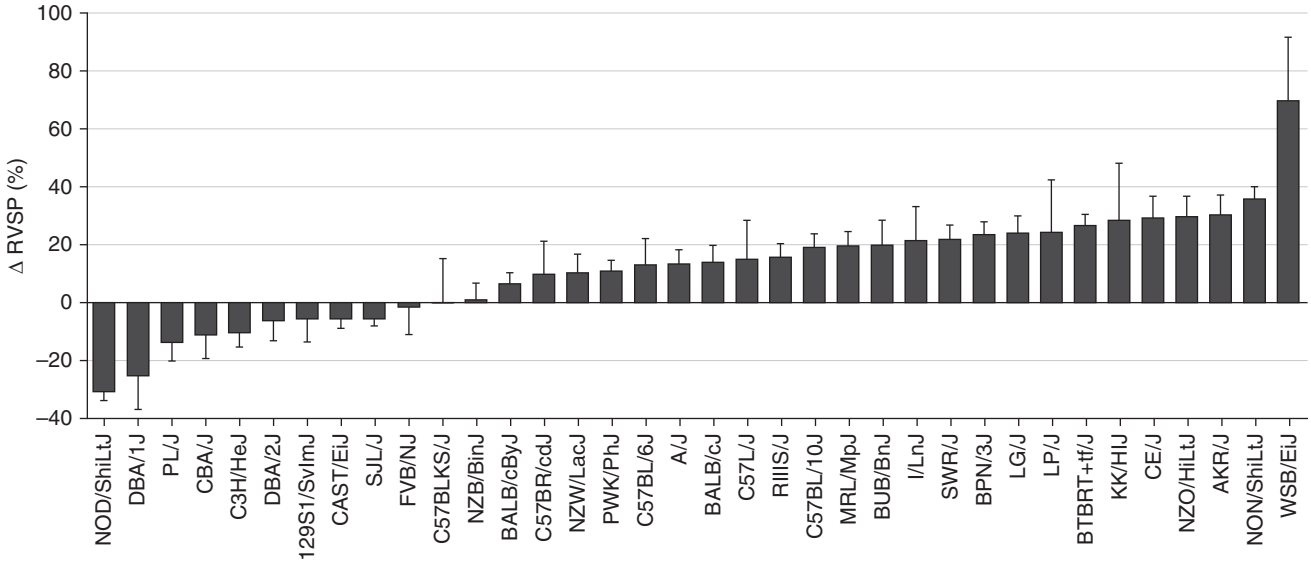

Figure 1. Response to high-fat diet (HFD)–induced pulmonary hypertension (PH) in 36 strains of mice; 36 inbred and wild-derived mouse strains were subjected to regular diet (RD; 15% lipids/kcal) or HFD (60% lipids/kcal) for 20 weeks. Percentage changes in right ventricular systolic pressure (RVSP) were calculated as the HFD value divided by the average RD value in each mouse strain. Data are mean (±SEM; $n = 3$–8 mice/diet per strain).

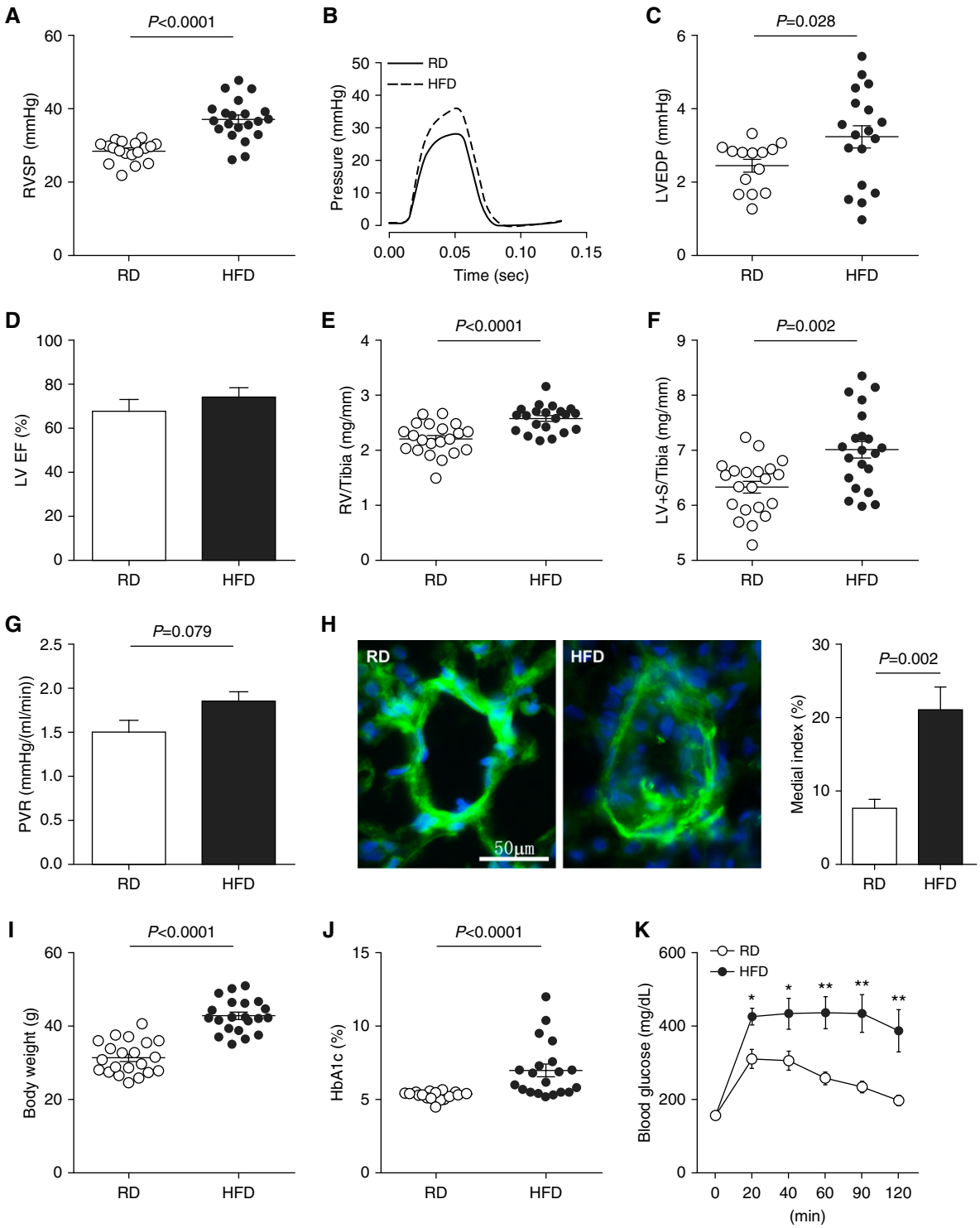

Figure 2. Validation of HFD-induced heart failure and preserved ejection fraction (PH-HFpEF) in AKR/J mouse. Male AKR/J mice (8 wk old) were exposed to RD and HFD for 16–20 weeks. (*A*) RVSP measured by right heart catheterization. (*B*) Representative RV pressure wave forms. (*C* and *D*) Left ventricular end-diastolic pressure (LVEDP) and LV ejection fraction (LVEF) measured by left heart catheterization. (*E* and *F*) RV and LV hypertrophy assessed by RV or LV weight over tibial length. (*G*) Pulmonary vascular resistance (PVR) measured in AKR/J mice fed with RD and HFD. (*H*) Representative images of lung sections stained with α-smooth muscle actin and quantification of medial index from the mean of 5–10 vessels per lung section from eight mice per group. *Scale bar*, 50 μm. (*I* and *J*) Body weights and HbA1c levels measured at the end of study. (*K*) Glucose tolerance test performed at Week 19. Data are mean (±SEM; $n = 14$ mice/group for glucose tolerance test; $^{*}P < 0.05$ and $^{**}P < 0.01$). S, septum.

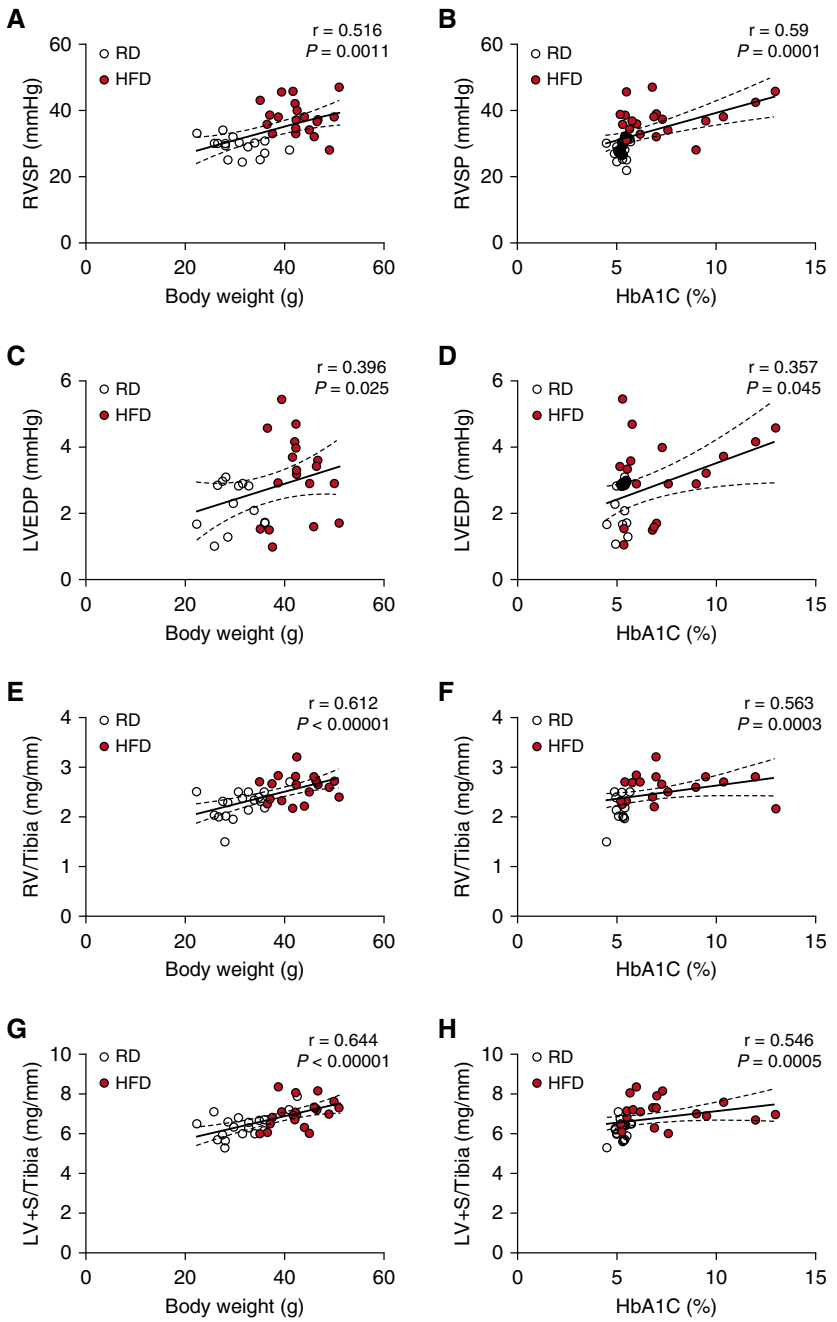

Figure 3. Dependence of RVSP, LVEDP, and biventricular hypertrophy on body weight and HbA1c in AKR/J mice. Correlation of body weight and RVSP (*A*), LVEDP (*C*), RV hypertrophy (RVH) (*E*), and LV hypertrophy (LVH) (*G*) in AKR/J mice. Correlation of HbA1c levels and RVSP (*B*), LVEDP (*D*), RVH (*F*), and LVH (*H*) in mice. Spearman *r* is shown.

the increased body weights and HbA1c levels, our data show increased RVSP with elevated LVEDP, as well as both RV and LV hypertrophy after 12 weeks of HFD (Figures 4C–4F). These results demonstrate that AKR/J mice subjected to HFD progressively develop metabolic syndrome–associated PH-HFpEF.

129S1/SvlmJ Is Resistant to HFD-Induced PH-HFpEF

Among the strains that are resistant to HFD-induced PH (Figure 1), we selected 129S1/SvlmJ mouse strain for further validation, because it is commonly used to generate genetically engineered mice. Whereas body weights, HbA1c levels, and glucose intolerance were increased in 129S1/SvlmJ mice after 20 weeks of HFD exposure compared with RD-treated mice (Figures 5A–5C), we observed no increase in RVSP (19.3 ± 0.9 and 20.4 ± 1 mm Hg, RD and HFD, respectively; Figure 5D), nor did we detect changes in LVEDP or biventricular hypertrophy in HFD-treated 129S1/SvlmJ mice (Figures 5F–5H). In addition, no significantly difference in RVSP was observed after 40 or 60 weeks of HFD exposure in 129S1/SvlmJ mice (21.8 ± 1.8 and 25 ± 1.4 mm Hg, RD and HFD, respectively, at Week 60; Figure 5I). Together, these data demonstrate that 129S1/SvlmJ is a highly resistant strain to HFD-induced PH-HFpEF.

Discussion

The development of PH in HFpEF has been increasingly recognized as a clinical complication of metabolic syndrome. However, there are no consensus therapeutic strategies and no genetically modifiable mouse models available for advancing our understanding of the molecular basis of metabolic syndrome–associated PH-HFpEF. Using high-fat feeding, which is a well described method to induce metabolic syndrome in mice, across 36 inbred and wild-derived mouse strains, we identified the inbred strain, AKR/J, as a mouse model of metabolic syndrome–associated PH-HFpEF. This HFD/AKR/J mouse model recapitulates key clinical features known to be present in patients with PH-HFpEF, including elevated RVSP and LVEDP, preserved LVEF, and biventricular hypertrophy. Moreover, this mouse model was further validated for the reliability and reproducibility in multiple experimental sets (Figure E1).

After 16–20 weeks of HFD exposure in AKR/J mice, we observed that an increase in severity of PH (~37 mm Hg) was close to that observed in patients with PH-HFpEF (RVSP range, 46–51 mm Hg) (5, 7). Although LVEDP levels in the HFD/AKR/J mice were lower compared with patients with PH-HFpEF, this may have been caused by intraoperative hemorrhage during invasive right-to-left-sided cardiac catheterization in animals, as well as prolonged anesthesia (left-sided pressures are obtained after RV measures in our

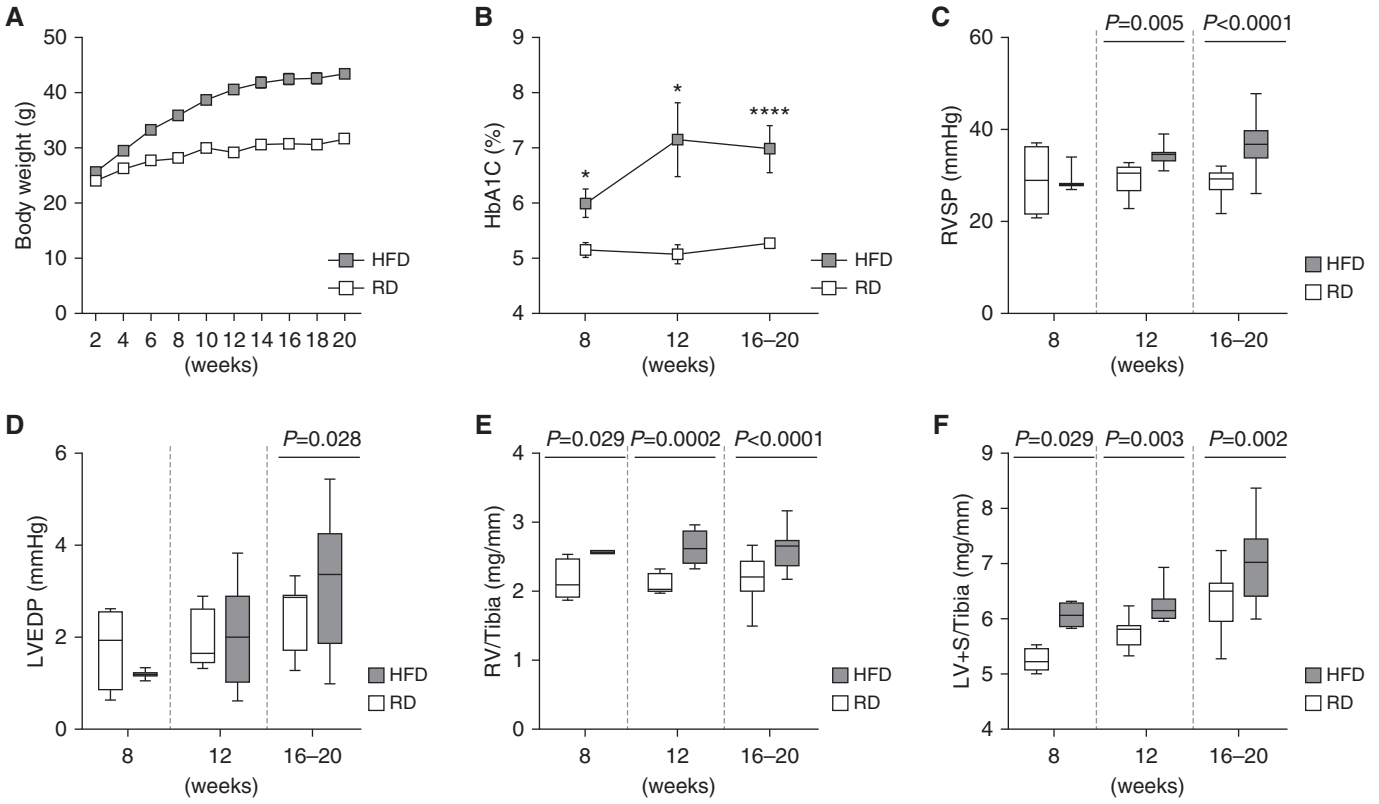

Figure 4. Progression of PH-HFpEF throughout the treatment of HFD in AKR/J mouse. Male AKR/J mice (8 wk old) were subjected to RD or HFD for the indicated time periods. (*A*) Body weights measured during a 20-week period. (*B*) HbA1c levels measured in whole-blood samples collected at Weeks 8, 12, and 20. (*C* and *D*) RVSP and LVEDP measured at Weeks 8, 12, and 20. Data are mean (±SEM). *$P < 0.05$ and ****$P < 0.0001$. (*E* and *F*) RV and LV hypertrophy assessed by RV or LV weight over tibial length at Weeks 8, 12, and 20. $n = 4$, 7, and 21 mice per group, respectively.

protocols). In agreement with the previous findings, which suggest that patients with PH-HFpEF have a high prevalence of obesity, diabetes, and hypertension (6, 15, 17), HFD/AKR/J mice also develop a diabetic phenotype associated with obesity and severe glucose intolerance. Interestingly, hemodynamic features of PH-HFpEF in HFD/AKR/J mice appear to correlate with elevated body weight and HbA1c levels (Figure 3), consistent with the previous findings that link obesity, hyperglycemia, and diabetes to increased LVEDP and elevated pulmonary pressures in patients with PH-HFpEF (5, 6, 17). Together, these data demonstrate that HFD/AKR/J mouse model is relevant to the pathogenesis and clinical outcomes of human PH-HFpEF.

Recently, our group has developed a two-hit model of PH-HFpEF, which combines SU5416-induced pulmonary endothelial injury in rats with multiple features of metabolic syndrome, diabetic nephropathy, and diastolic dysfunction (obese ZSF1) (18). This rat model was used to evaluate the therapeutic effects of both metformin and sodium nitrite on insulin sensitivity and PH. Both agents improved metabolic syndrome via the activation of sirtuin-3 in skeletal muscle, which signaled via AMP-activated protein kinase and glucose transporter type 4 to increase skeletal muscle glucose uptake. Both agents reduced pulmonary pressure in early intervention models, suggesting new approaches to PH-HFpEF therapy. Although AKR/J mice present a less profound diabetic phenotype after 20-week exposure to HFD, we found that pulmonary pressures in both SU5416/obese ZSF1 rats and HFD/AKR/J mice increase to the same degree, which was accompanied by similar increases in LVEDP, RV hypertrophy, and LV hypertrophy. Moreover, consistent with our previous finding in SU5416/obese ZSF1 rats, chronic oral supplementations of nitrite and metformin also significantly reduced pulmonary pressures in HFD/AKR-J mice (Figure E3). Hence, the similarities between these two animal models imply that the HFD/AKR/J mouse model of metabolic syndrome–associated PH-HFpEF can be employed broadly, notably, when gene manipulations are required.

Although we observed that 129S1/SvlmJ and AKR/J mice had similar levels of obesity and glucose intolerance after 20 weeks of HFD exposure, 129S1/SvlmJ mice had lower HbA1c levels and were correspondingly resistant to HFD-induced PH. This observation may be explained by previous findings, where 129-background mice had high high-density lipoprotein cholesterol levels and normal insulin sensitivity when fed with an HFD (26, 27). Interestingly, even though HFD-treated C57BL/6J and AKR/J mice developed a comparable degree of obesity, glucose intolerance, and hyperglycemia (Figure E4), changes in RVSP were moderate in C57BL/6J mice. The mechanism leading to this difference is unclear; however, HFD-treated C57BL/6J mice have been reported to have less severe insulin resistance compared with AKR/J mice (28). Recently, high-fat, high-sucrose diet has been shown to induce profound

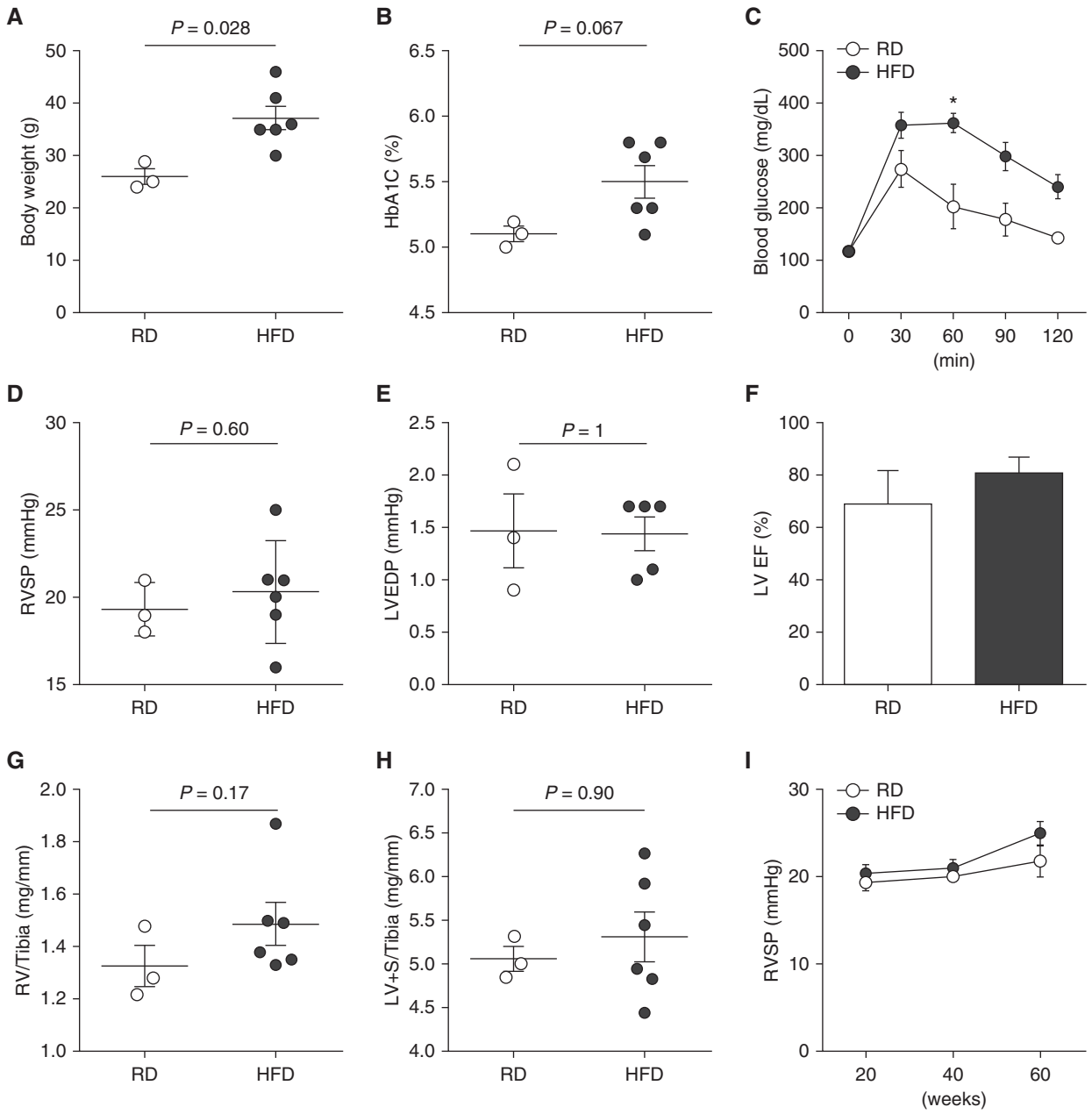

Figure 5. 129S1/SvImJ is resistant to HFD-induced PH-HFpEF. Male 129S1/SvImJ mice (8-wk-old) were exposed to RD or HFD. (*A* and *B*) Body weights and HbA1c levels measured at Week 20. (*C*) Glucose tolerance test performed with an intraperitoneal injection of dextrose (1.8 mg/g) at Week 19. (*D*, *E*, and *F*) RVSP, LVEDP, and LVEF measured at Week 20. (*G* and *H*) RV and LV hypertrophy determined by RV or LV weight over tibial length at Week 20. (*I*) RVSP measured after 20, 40, and 60 weeks of exposure to RD or HFD. Data are mean (±SEM; $n = 3$–6 mice per group; $^*P < 0.05$).

mitochondrial dysfunction and insulin resistance in C57BL/6J mice (29). It is possible that a second hit of high sucrose or SU5416 may exacerbate insulin resistance or endothelial injury, thus predisposing HFD-treated C57BL/6J mice to PH and/or PH-HFpEF; however, further experiments are needed. Moreover, we are intrigued by the extremely different response to HFD-induced PH in NOD/shiLtJ and NON/shiLtJ strains, which share similar genetic background and are both widely used for diabetes research. NOD/ShiLtJ mice develop autoimmune type I diabetes (30), and it is the most resistant strain to HFD-induced PH across all 36 mouse strains tested. In contrast, the NON/shiLtJ mouse strain is known to be sensitive to HFD-induced obesity and type II diabetes, and was highly susceptible to HFD-induced PH. It is also reported that NON/shiLtJ mice develop more severe obesity and insulin resistance than C57BL/6J mice (31). Hence, these data suggest that the severe insulin-resistant phenotype and the appearance of type II diabetes are important pathophysiological abnormalities, which predispose to metabolic syndrome–associated PH-HFpEF. It may be interesting for

researchers to tease out whether these criteria will differ in prognosis and predicting the progression of PH-HFpEF in future epidemiological studies. Furthermore, in an accompanying evaluation of genome-wide association, Kelly and colleagues (22) identify candidate genes that regulate RVSP across all 36 strains.

In summary, our HFD/AKR/J mouse model offers a new avenue for identifying mechanisms and potential targets for therapeutic intervention for this disease. The use of effective treatments approved for PAH has been shown to be inefficient or even harmful in patients with PH-HFpEF. Because there is no approved specific therapy and no consensus therapeutic strategy for PH-HFpEF at present, the development of a genetically modifiable HFD/AKR/J mouse model that recapitulates key clinical features known to be present in patients with PH-HFpEF is important for future work in the field. ■

Author disclosures are available with the text of this article at www.atsjournals.org.

Acknowledgments: The authors thank Dr. Sergei Snovida for helpful comments on the manuscript and Eugene Lapshin and Christine Burton (University of Pittsburgh, Pittsburgh, PA) for technical assistance.

References

1. Simonneau G, Robbins IM, Beghetti M, Channick RN, Delcroix M, Denton CP, Elliott CG, Gaine SP, Gladwin MT, Jing ZC, *et al*. Updated clinical classification of pulmonary hypertension. *J Am Coll Cardiol* 2009;54(1 suppl):S43–S54.
2. Hogg K, Swedberg K, McMurray J. Heart failure with preserved left ventricular systolic function; epidemiology, clinical characteristics, and prognosis. *J Am Coll Cardiol* 2004;43:317–327.
3. Damy T, Goode KM, Kallvikbacka-Bennett A, Lewinter C, Hobkirk J, Nikitin NP, Dubois-Randé JL, Hittinger L, Clark AL, Cleland JG. Determinants and prognostic value of pulmonary arterial pressure in patients with chronic heart failure. *Eur Heart J* 2010;31:2280–2290.
4. Delgado JF, Conde E, Sánchez V, López-Ríos F, Gómez-Sánchez MA, Escribano P, Sotelo T, Gómez de la Cámara A, Cortina J, de la Calzada CS. Pulmonary vascular remodeling in pulmonary hypertension due to chronic heart failure. *Eur J Heart Fail* 2005;7: 1011–1016.
5. Leung CC, Moondra V, Catherwood E, Andrus BW. Prevalence and risk factors of pulmonary hypertension in patients with elevated pulmonary venous pressure and preserved ejection fraction. *Am J Cardiol* 2010; 106:284–286.
6. Thenappan T, Shah SJ, Gomberg-Maitland M, Collander B, Vallakati A, Shroff P, Rich S. Clinical characteristics of pulmonary hypertension in patients with heart failure and preserved ejection fraction. *Circ Heart Fail* 2011;4:257–265.
7. Klapholz M, Maurer M, Lowe AM, Messineo F, Meisner JS, Mitchell J, Kalman J, Phillips RA, Steingart R, Brown EJ Jr, *et al*.; New York Heart Failure Consortium. Hospitalization for heart failure in the presence of a normal left ventricular ejection fraction: results of the New York Heart Failure Registry. *J Am Coll Cardiol* 2004;43: 1432–1438.
8. Gerges M, Gerges C, Pistritto AM, Lang MB, Trip P, Jakowitsch J, Binder T, Lang IM. Pulmonary hypertension in heart failure: epidemiology, right ventricular function, and survival. *Am J Respir Crit Care Med* 2015; 192:1234–1246.
9. Vanderpool RR, Gladwin MT, Simon MA. Hemodynamic markers of pulmonary vascular disease in pulmonary hypertension due to left heart disease [abstract]. *J Heart Lung Transplant* 2015;34: S118.
10. Lloyd-Jones D, Adams R, Carnethon M, De Simone G, Ferguson TB, Flegal K, Ford E, Furie K, Go A, Greenlund K, *et al*.; American Heart Association Statistics Committee and Stroke Statistics Subcommittee. Heart disease and stroke statistics—2009 update: a report from the American Heart Association Statistics Committee and Stroke Statistics Subcommittee. *Circulation* 2009;119: e21–e181. [Published erratum appears in *Circulation* 119:480–486.]
11. Oktay AA, Rich JD, Shah SJ. The emerging epidemic of heart failure with preserved ejection fraction. *Curr Heart Fail Rep* 2013;10: 401–410.
12. Cappola TP, Felker GM, Kao WH, Hare JM, Baughman KL, Kasper EK. Pulmonary hypertension and risk of death in cardiomyopathy: patients with myocarditis are at higher risk. *Circulation* 2002;105: 1663–1668.
13. Lam CS, Roger VL, Rodeheffer RJ, Borlaug BA, Enders FT, Redfield MM. Pulmonary hypertension in heart failure with preserved ejection fraction: a community-based study. *J Am Coll Cardiol* 2009;53: 1119–1126.
14. Abramson SV, Burke JF, Kelly JJ Jr, Kitchen JG III, Dougherty MJ, Yih DF, McGeehin FC III, Shuck JW, Phiambolis TP. Pulmonary hypertension predicts mortality and morbidity in patients with dilated cardiomyopathy. *Ann Intern Med* 1992;116: 888–895.
15. Guazzi M. Pulmonary hypertension in heart failure preserved ejection fraction: prevalence, pathophysiology, and clinical perspectives. *Circ Heart Fail* 2014;7:367–377.
16. Shapiro BP, McGoon MD, Redfield MM. Unexplained pulmonary hypertension in elderly patients. *Chest* 2007;131:94–100.
17. Robbins IM, Newman JH, Johnson RF, Hemnes AR, Fremont RD, Piana RN, Zhao DX, Byrne DW. Association of the metabolic syndrome with pulmonary venous hypertension. *Chest* 2009;136: 31–36.
18. Lai YC, Tabima DM, Dube JJ, Hughan KS, Vanderpool RR, Goncharov DA, St Croix CM, Garcia-Ocaña A, Goncharova EA, Tofovic SP, *et al*. Sirt3-AMP–activated protein kinase activation by nitrite and metformin improves hyperglycemia and normalizes pulmonary hypertension associated with heart failure with preserved ejection fraction. *Circulation* 2016;133:717–731.
19. Kelly N, Fitch A, Michael H, Ghedin E, Tipton L, Lucht L, Gladwin MT, Shapiro SD, Morris AM. Susceptibility to high-fat diet–induced pulmonary hypertension is associated with reduced gi alpha-diversity and altered species composition in mice [abstract]. *Am J Respir Crit Care Med* 2015;191:A3961.
20. Kelly N, Radder J, Baust J, Burton C, Agostini B, Wood J, Gregory A, Leme A, Shapiro SD. Genome-wide association study with interactome-based scoring identifies dok4 and ppp2ca as novel candidate genes in high-fat diet-induced pulmonary hypertension [abstract]. *Am J Respir Crit Care Med* 2016;193: A2219.
21. Meng Q, Bueno M, Kelly N, Lai YC, Mora AL, Gladwin MT. Evaluation of the therapeutic effects of nitrite and metformin in a mouse model of pulmonary hypertension associated with heart failure and preserved ejection fraction [abstract]. *Am J Respir Crit Care Med* 2016;193: A3888.
22. Kelly NJ, Radder JE, Baust JJ, Burton CL, Lai YC, Potoka KC, Agostini BA, Wood JP, Bachman TN, Vanderpool RR, *et al*. Mouse Genome–Wide Association Study of preclinical Group II pulmonary hypertension identifies epidermal growth factor receptor. *Am J Respir Cell Mol Biol* 2017;56: 488–496.
23. Hansmann G, Wagner RA, Schellong S, Perez VA, Urashima T, Wang L, Sheikh AY, Suen RS, Stewart DJ, Rabinovitch M. Pulmonary arterial hypertension is linked to insulin resistance and reversed by peroxisome proliferator-activated receptor-γactivation. *Circulation* 2007;115:1275–1284.
24. Kelley EE, Baust J, Bonacci G, Golin-Bisello F, Devlin JE, St Croix CM, Watkins SC, Gor S, Cantu-Medellin N, Weidert ER, *et al*. Fatty acid nitroalkenes ameliorate glucose intolerance and pulmonary hypertension in high-fat diet–induced obesity. *Cardiovasc Res* 2014;101:352–363.

25. Alexander J, Chang GQ, Dourmashkin JT, Leibowitz SF. Distinct phenotypes of obesity-prone AKR/J, DBA2J and C57BL/6J mice compared to control strains. *Int J Obes* 2006; 30:50–59.
26. Ussar S, Fujisaka S, Kahn CR. Interactions between host genetics and gut microbiome in diabetes and metabolic syndrome. *Mol Metab* 2016;5:795–803.
27. Ishimori N, Li R, Kelmenson PM, Korstanje R, Walsh KA, Churchill GA, Forsman-Semb K, Paigen B. Quantitative trait loci that determine plasma lipids and obesity in C57BL/6J and 129S1/SvImJ inbred mice. *J Lipid Res* 2004;45:1624–1632.
28. Rossmeisl M, Rim JS, Koza RA, Kozak LP. Variation in type 2 diabetes—related traits in mouse strains susceptible to diet-induced obesity. *Diabetes* 2003;52:1958–1966.
29. Bonnard C, Durand A, Peyrol S, Chanseaume E, Chauvin MA, Morio B, Vidal H, Rieusset J. Mitochondrial dysfunction results from oxidative stress in the skeletal muscle of diet-induced insulin-resistant mice. *J Clin Invest* 2008;118:789–800.
30. Atkinson MA, Leiter EH. The NOD mouse model of type 1 diabetes: as good as it gets? *Nat Med* 1999;5:601–604.
31. O'Brien PD, Sakowski SA, Feldman EL. Mouse models of diabetic neuropathy. *ILAR J* 2014;54:259–272.